The dynamic behaviour of solids in incremental nonlinear elasticity: perturbations and integral equations

Davide Bigoni
Dipartimento di Ingegneria Meccanica e Strutturale, Università di Trento, Italy
E-mail: *bigoni@ing.unitn.it*

Domenico Capuani
Dipartimento di Architetura, Università di Ferrara, Italy
E-mail: *d.capuani@unife.it*

Keywords: nonlinear elasticity, pre-stressed solids, singular fundamental solution, shear bands

SUMMARY: The dynamic behaviour of pre-stressed, elastic orthotropic and incompressible materials is considered in the time-harmonic regime. Depending on the level of pre-stress and anisotropy, wave patterns are shown to emerge, with focussing of signals in the direction of shear bands. Varying the direction of the dynamic perturbation excites different wave patterns, which tend to degenerate to families of plane waves parallel to the shear bands, when the elliptic boundary is approached. Integral representations have been obtained by Bigoni and Capuani (2005).

1. INTRODUCTION

The dynamic behaviour of pre-stressed, elastic orthotropic and incompressible materials is considered in the time-harmonic regime. In the Biot [1965] constitutive framework, infinite-body, dynamic Green's functions and boundary integral equations for incremental displacements and in-plane incremental hydrostatic stress, have been obtained by the authors (Bigoni and Capuani, 2005) for small, isochoric and two-dimensional deformation superimposed upon a given nonlinear elastic and homogeneous strain. Due to the hypothesis of time-harmonic deformation, the regime classification of the governing differential equations remains identical to the quasi-static case, so that all obtained solutions lie within the elliptic range. A perturbation in terms of a pulsating dipole can be therefore obtained and employed to analyse material instabilities arising near the boundary of ellipticity loss. The perturbative approach is general since it can be employed for any incrementally linear constitutive equation, dynamic loadings and inhomogeneous material (Willis [1991]) and is capable of revealing aspects which may remain undetected using methods for material instabilities based on weak discontinuity surfaces (loss of ellipticity, e.g. Knowles and Sternberg, 1978). For instance, the perturbative approach has revealed shear band formation for a Mooney-Rivlin material in the quasi-static case (Bigoni and Capuani, 2002, their Fig. 3), a circumstance confirmed by the present dynamic analysis, but not detected by the conventional approach.

Results presented in the present work provide a basis for the analysis of propagation of dynamic disturbances near the boundary of loss of ellipticity. Depending on the level of pre-stress and anisotropy, wave patterns are shown to emerge, with focussing of signals in the direction of shear bands. Varying the direction of the dynamic perturbation excites different wave patterns, which tend to

degenerate to families of plane waves parallel to the shear bands, when the elliptic boundary is approached.

Another possibility related to the finding of a Green's function is the formulation of a boundary element technique for the solution of incremental boundary value problems. For quasi-static deformation, this technique was proved to possess certain advantages related for instance to the treatment of the incompressibility constraint with respect to other numerical techniques, such as finite element methods. Now the development of the technique in dynamics requires the finding of new boundary integral equations. While the integral equation for incremental displacements does not formally change with respect to the quasi-static case, a generalization of the integral representation for incremental in-plane hydrostatic stress has been obtained by Bigoni and Capuani (2005). The reader is referred to this paper for the framework of equations.

2. WAVE PROPAGATION AND SHEAR BANDS

Employing self-equilibrated combinations of concentrated forces, Bigoni and Capuani (2002) provided a perturbative approach to material instability analyzed within the boundary of loss of ellipticity. In particular, the simplest perturbing system was employed, consisting of a dipole (two equal and opposite forces), acting on a pre-stressed, infinite medium. This approach is general, so that it applies to any incrementally linear constitutive equation and allows for investigation of situations, such as inhomogeneous materials or dynamic loadings, where instability criteria based on weakly discontinuous surface may be in a sense "opaque". As examples of such situations, we may mention the cases of Mooney-Rivlin, which will be confirmed here to display shear band pattern formation for dynamic disturbances, and of flutter instability, a situation which may occur when the constitutive equations lack major symmetry and which remains unexplored using the conventional approach.

Similarly to the quasi-static case, a time-harmonic pulsating dipole is used as a perturbing agent, acting on a pre-stressed infinite medium. μ and μ^* are two incremental moduli, denoting respectively the moduli corresponding to shearing parallel to, and at 45° to, the principal stress axes, and k is a dimensionless pre-stress parameter ($k=\sigma/2\mu$) The effect of the dynamic perturbation decays with distance, but the decay becomes slower and slower in a path (in the k vs. μ^*/μ space) towards the boundary of ellipticity. The interesting feature is represented by the deformation patterns emerging when the loss of ellipticity is approached.

We begin with the simple example of a Mooney-Rivlin material (in our case of plane strain deformation this material model coincides with a neo-Hookean material) for which

$$\sigma = \mu_0 (\lambda^2 - \lambda^{-2}), \qquad \mu_* = \mu = \frac{\mu_0}{2}(\lambda^2 + \lambda^{-2}), \qquad k = \frac{\lambda^4 - 1}{\lambda^4 + 1} \tag{1}$$

where $\lambda > 1$ is the maximum current stretch and μ_0 is a shear modulus in an initial state. Ellipticity would be lost in the above material when $k = 1$, corresponding to the unphysical situation of infinite stretch. For this material, shear band formation in the sense of emergence of discontinuity surfaces remains excluded.

Level sets of the modulus of the real (left in the figure) and imaginary (right in the figure) parts of the Green's function for incremental displacements [nondimensionalized through multiplication by μ]

are represented in the figures, in a region defined by the non-dimensional coordinates x_1/a and x_2/a, where $2a$ is the distance between two unit forces defining the dipole. Unless otherwise specified, the dipole is centred at the origin and aligned parallel to the x_1-axis. Figs. 1-3, pertaining to Mooney-Rivlin material, are relative to different values of the pre-stress parameter k. In particular, k = 0 [or λ=1 from eqn. (1)], for Fig. 1; k = 0.5 [or λ=1.316 from eqn. (1)], for Fig. 2; and k = 0.98 [or λ=3.154 from eqn. (1)], for Fig. 3.

In the quasi-static case, the displacement maps plotted in the dimensionless coordinates x_1/a and x_2/a become independent of the dipole distance a. This is not true in the dynamic case: the solution now depends on the dimensionless scale parameter

$$\frac{a\Omega}{c} = \frac{a2\pi}{\lambda_1} \tag{2}$$

where λ_1 corresponds to the wavelength of a plane wave propagating parallel to the x_1-axis. Therefore, parameter (2) can be viewed as a measure of the perturbation wavelength related to the distance between the two forces forming the dipole.

The effects related to the changes in parameter (2) are systematically investigated, so that different parts of the same figures correspond (unless otherwise specified) to different values of the parameter. In particular, all upper parts of Figs. 1-3 refer to a low frequency limit, $a\Omega/c = \pi/100$, so that the real part is coincident with the quasi-static solution reported by Bigoni and Capuani (2002, their Fig. 3). The central parts of the figures correspond to $a\Omega/c = \pi/4$ and the lower parts to $a\Omega/c = \pi$. Compared to Fig.1, we note anisotropy effects in Fig. 2, where shear banding is not yet visible. However, the anisotropy dramatically affects the propagation in Fig.3, where k = 0.98, a value relatively close to the loss of ellipticity. Here shear band emergence interacts with wave propagation, creating a strong orientation (shear bands become horizontal at the EI boundary) and focussing of the signal, which tends to propagate only in the horizontal direction. The effect increases with frequency, so that at $a\Omega/c = \pi$. the width of shear bands becomes so narrow that the definition of the plot is not sufficient to visualize displacement patterns, at least at the same scale of the other figures. In this case, the signal almost does not propagate and therefore the displacement map remains prevailingly dark. Specifically, the propagation speeds in a Mooney-Rivlin material (1) for plane waves travelling parallel to axes x1 and x2 are $\lambda\,(\mu_0/\rho)^{1/2}$ and $(\mu_0/\rho)^{1/2}/\lambda$, respectively. The former tends to infinity and the latter to zero when the elliptic boundary is approached. In the particular case of $a\Omega/c = \pi/4$ and k = 0.98, the wavelengths characterizing propagation parallel to axes x_1 and x_2 are 8a and 0.80a, respectively. The wavelength in the direction x_2 is visible in the central part of Fig. 3 (where distance between peaks correspond to one half of the wavelengths), whereas those along x1-axis become visible in Fig. 4, which is an extension of Fig. 3 with x_1/a ranging between 0 and 20. This figure shows that wave patterns emanating from the dipole have an elliptical shape, whose aspect ratio depends on the pre-stress parameter k. At increasing distance from the dipole, the disturbances tend to propagate as plane waves travelling parallel to the x2-axis. Moreover, the elliptical shapes tend to self-similarly decrease for increasing values of $a\Omega/c$, thus explaining the "shadowing effect" visible in the lower part of Fig. 3.

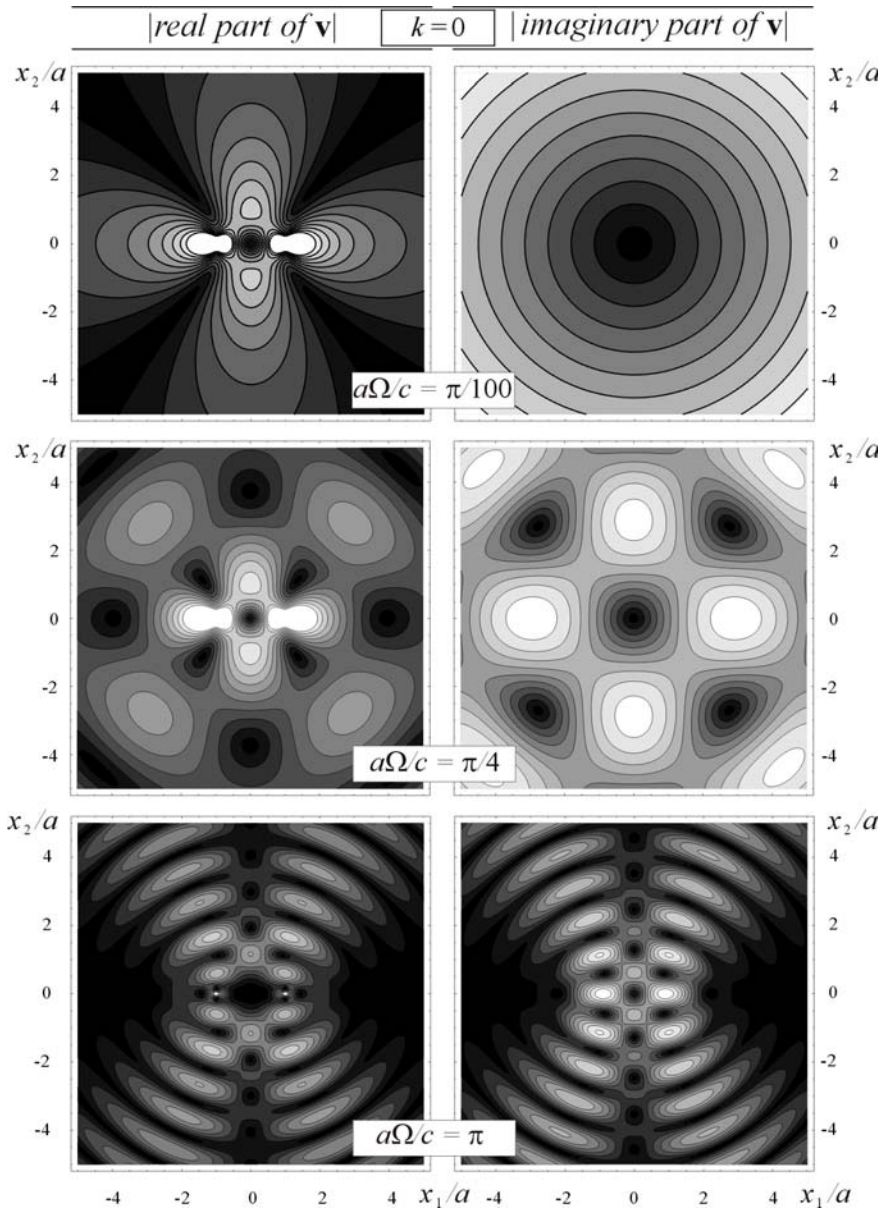
|real part of v|
k = 0
|imaginary part of v|
x2/a
x1/a
aΩ/c = π/100
aΩ/c = π/4
aΩ/c = π
4
2
0
-2
-4

Figure 1

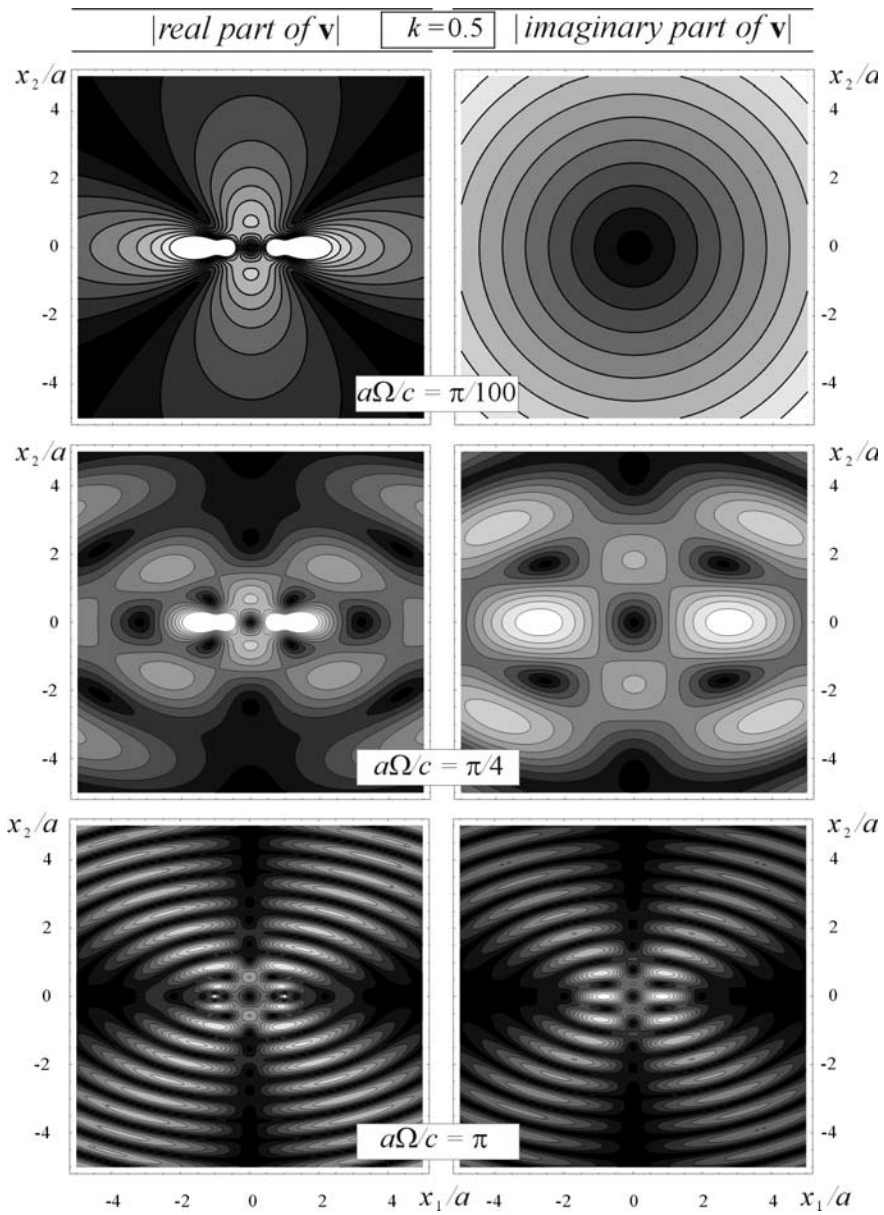
|real part of v|
k = 0.5
|imaginary part of v|
x2/a
x1/a
aΩ/c = π/100
aΩ/c = π/4
aΩ/c = π
4
2
0
-2
-4

Figure 2

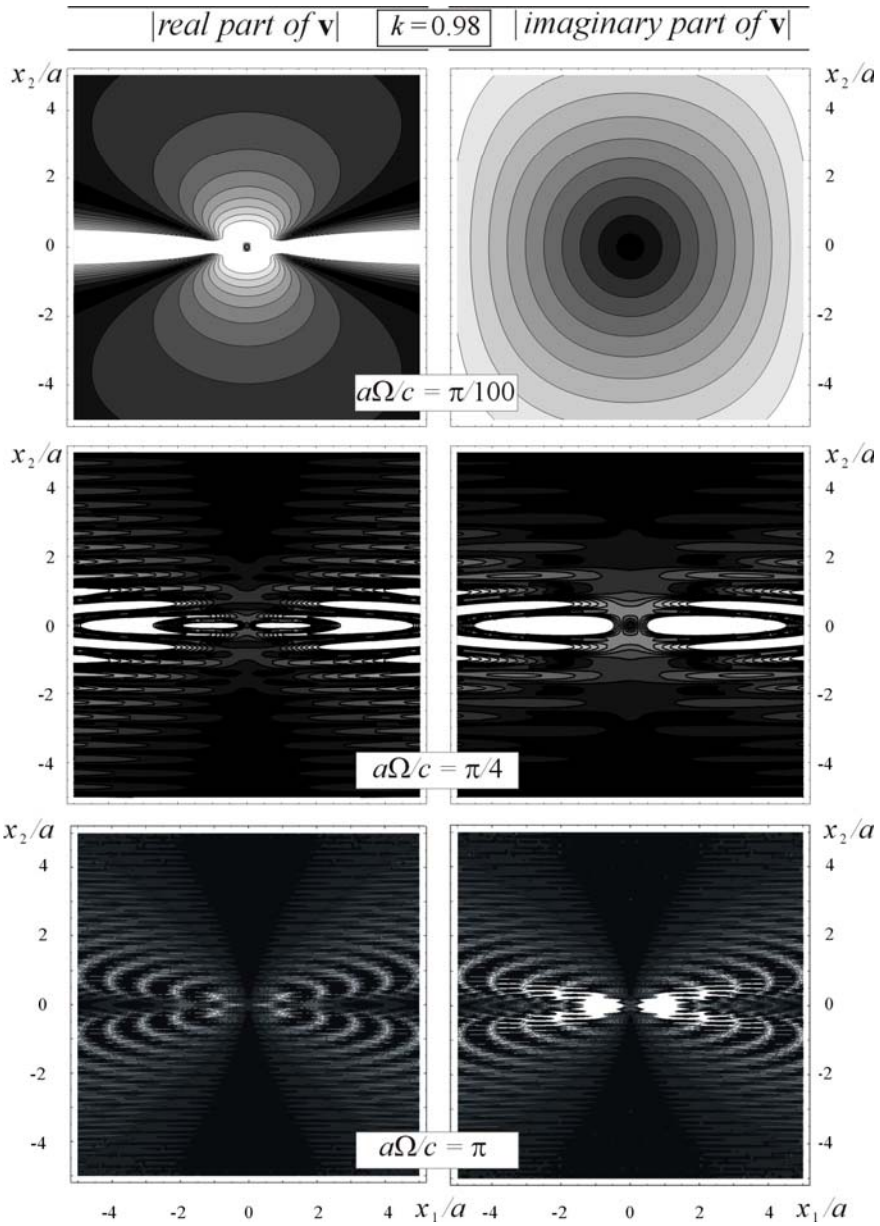
|real part of v|
k = 0.98
|imaginary part of v|
x2/a
x1/a
aΩ/c = π/100
aΩ/c = π/4
aΩ/c = π
4
2
0
-2
-4

Figure 3

Although restricted to plane, incompressible elasticity, it is considered unlikely that the above conclusions are specific to the assumed constitutive model. Rather, we believe that the above approach opens a new perspective to the analyses of material instability.

References:

Biot, M.A. (1965), *Mechanics of Incremental Deformations*, J. Wiley & Sons, New York.

Bigoni D., Capuani D. (2002), "Green's function for incremental nonlinear elasticity: shear bands and boundary integral formulation", *Journal of the Mechanics and Physics of Solids*, **50**, 471-500.

Bigoni D., Capuani D. (2005), "Time-harmonic Green's function and boundary integral formulation for incremental nonlinear elasticity: dynamics of wave patterns and shear bands", *Journal of the Mechanics and Physics of Solids*, **53**, 1163-1187.

Knowles J.K., Sternberg E. (1978), "On the failure of ellipticity and the emergence of discontinuous deformation gradients in plane finite elastostatics", *Journal of Elasticity*, **8**, 329-379.

Willis, J.R. (1991), "Inclusions and cracks in constrained anisotropic media", in *Modern Theory of Anisotropic Elasticity and Applications* (Wu J.J., Ting T.C.T., Barnett D.M., Eds.) SIAM, Philadelphia, 87-102.